DIVISION S-6—SOIL & WATER MANAGEMENT & CONSERVATION

Soil Aggregate and Texture Effects on Suspension Components from Wind Erosion

N. Mirzamostafa, L. J. Hagen,* L. R. Stone, and E. L. Skidmore

ABSTRACT

Many detrimental impacts are caused by the suspension-size (<0.10-mm) dust (SSD) generated during wind erosion. Prediction models of SSD are needed to assess SSD magnitudes and also aid in design of controls. Current models tend to lump together all sources of SSD from the soil surface, and their overall structure is best suited for use on large, uniform source areas. We reviewed equations developed to simulate generation of SSD on a subfield scale from individual structural components of the soil. These sources include direct emission of loose SSD, abrasion of SSD from surface clods by impacting saltating aggregates, and breakdown of saltating soil aggregates to SSD. The main objective of this study was to experimentally determine the effects of aggregate structure and soil texture on the individual SSD sources for a range of Kansas soils. Periodic sampling of 11 soils showed that the fraction of loose SSD in the upper 20 mm available for emission ranged from 0.7 to 80% of soil mass. However, variation in the mean SSD fraction in these soils was directly related to soil texture (r^2 = 0.87). Content of SSD in the total mass abraded from clods in a wind tunnel ranged from 14 to 27%. This range was relatively narrow, but related to parent soil clay content (r^2 = 0.69). Saltation-size aggregates were about nine times more stable than target clods of the same soils. However, the production of SSD based on breakage coefficients of saltating aggregates was also related to clay content of the parent soils (r^2 = 0.96).

WIND EROSION is a significant problem on agricultural lands throughout the USA as well as in many parts of the world (Oldeman, 1991). Wind erosion is particularly severe in arid and semiarid areas, which constitute one-third of the world's total land area and include about one-sixth of the world's population (Dregne, 1976; Gore, 1979). In the USA, wind erosion is the dominant problem on >28 million ha of land area. In the Great Plains, where severe wind erosion occurs, total land damaged annually ranges from 0.5 million to 6.0 million ha (U.S. Department of Agriculture, 1989).

Many detrimental impacts from wind erosion are caused by the SSD generated during erosion events. Adverse effects include depletion of soil fertility, visibility reduction leading to airport closures and road accidents, contamination of food and drinking water, air pollution, and economic losses (Clark et al., 1985; Hagen and Lyles, 1985; Lyles and Tatarko, 1986; Piper, 1989; Pye, 1987; Zobeck and Fryrear, 1986). The finest portion of SSD with an aerodynamic diameter of <10 μm (PM_{10}) is regulated as a human health hazard in the USA. Initial studies show wind erosion can generate significant amounts of PM_{10} from Kansas soils (Hagen et al., 1996), as well as from soils in other areas (Cahill et al., 1996).

To improve prediction of on-site and off-site erosion impacts, the suspension component of wind erosion needs to be quantified. Although many have studied transport and deposition of fine particles (e.g., Pye, 1987), few have studied the specific sources and magnitude of the total SSD component created during wind erosion.

Two main methods have been employed to estimate dust generation by wind erosion. One is use of the USDA Wind Erosion Equation (WEQ; Woodruff and Siddoway, 1965) to estimate total soil loss and then assign a fraction of that loss as dust generated by wind erosion (California Air Resources Board, 1991). Currently, the WEQ is the most widely used method for predicting average annual soil loss by wind from agricultural fields and for designing control practices. The WEQ is an empirical equation, however, so it is difficult to extend its use beyond regions where is has been calibrated.

A second approach has been to use an equation of the following general form:

$$F_D = f(A)f(q)^p \quad [1]$$

where F_D refers to a vertical dust flux (kg m^{-2} s^{-1}), which is generally some portion of the total suspended dust component, such as PM_{10}, or <0.02 mm (Gillette, 1977), or the portion <0.06 mm, which engages in long-range transport (Marticorena et al., 1997).

The function $f(q)$ represents a horizontal discharge near the surface (kg m^{-1} s^{-1}) and may include all of the horizontal discharge (Gillette, 1977). However, most recent models (Shao et al., 1996; Marticorena and Bergametti, 1995) have restricted $f(q)$ to only the saltation discharge in recognition of the significance of particle impacts in driving the dust generation process. The value of $f(q)$ may be raised to an empirical power, p. Typically, modelers have selected p equal to one, but based on a suggestion of Owen, a value greater than one also has been used (Gillette and Passi, 1988). The dimensional

N. Mirzamostafa and L.R. Stone, Dep. of Agronomy, Throckmorton Hall, Kansas State Univ., Manhattan, KS 66506; L.J. Hagen and E.L. Skidmore, USDA-ARS Wind Erosion Research Unit, Throckmorton Hall, Kansas State Univ., Manhattan, KS 66506. Contribution from USDA-ARS in cooperation with the Kansas Agric. Exp. St., Contribution no. 97-206-J. Received 24 Feb. 1997. *Corresponding author (hagen@weru.ksu.edu).

Published in Soil Sci. Soc. Am. J. 62:1351–1361 (1998).

Abbreviations: PM_{10}, dust with an aerodynamic diameter of <10 μm; SSD, suspension-size dust; WEPS, Wind Erosion Prediction System; WEQ, Wind Erosion Equation.

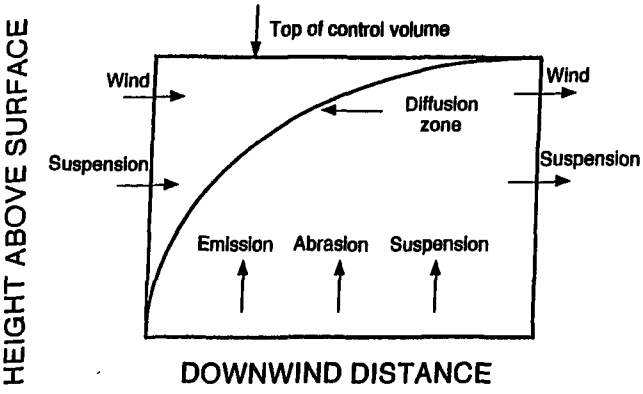

Fig. 1. Schematic of a control volume for the suspension component of the WEPS EROSION submodel (Hagen, 1995).

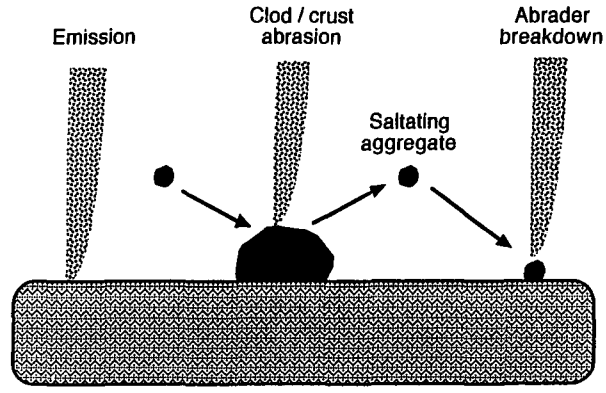

Fig. 2. Sources of suspension-size particles during wind erosion.

generation function, $f(A)$, has been used both as a constant (Gillette and Passi, 1988) and as a variable dependent on either aggregate-size distribution (Shao et al., 1996) or clay content (Marticorena and Bergametti, 1995).

In general, Eq. [1] has been applied to large source areas, with only minimal inputs of surface conditions by users. Equation [1] could also be applied at the individual field scale. But, because it treats the soil as a lumped source of SSD, it has little potential to allow updating surface conditions in response to wind erosion. It also ignores the effect of nonerodible field boundaries on SSD generation, which is probably significant on small fields.

In order to improve understanding of SSD generation at the individual field scale, this study on the suspension flux from wind erosion was carried out as part of a larger project that seeks to develop a new Wind Erosion Prediction System (WEPS). The overall objective of the project was to develop replacement technology for the WEQ (Hagen, 1991a).

In the WEPS, a mass conservation equation is used to calculate the suspension fraction of soil loss (Fig. 1). The suspension sources contribute SSD to successive, individual control volumes and are then advected downwind. In addition, the vertical suspension flux predicted by various source terms changes with both surface conditions and saltation discharge rates in successive downwind control volumes. Trapping of the suspension component is assumed negligible, except over nonerodible surfaces that may serve as sinks.

An examination of wind erosion processes led to the hypothesis that SSD produced during wind erosion comes from three possible sources (Fig. 2). The first source is emission of small soil aggregates that are already in the SSD range, which move directly into suspension. The second source is from the abrasion of surface clods and crust by impacting saltating aggregates. The third source is from breakdown of soil aggregates as they move in saltation. Assessment of these individual sources appears essential to improve estimates of the contributions of various soils to SSD during wind erosion events. We examined quasi-steady-state equations designed to simulate SSD generated by individual soil structural components on a subfield scale. The major objective of this study was to experimentally determine the effects of soil structure and texture on the individual SSD sources in a range of Kansas soils. The results of this study, combined with others, will be used in WEPS to predict the suspension component of wind erosion.

THEORY

First, a qualitative overview of the soil structure representation used in WEPS is presented, and then equations to simulate the suspension component that are compatible with that structure are discussed. Two basic structural states of bare field soils are simulated in WEPS (Hagen, 1995). After tillage, a typical surface may be composed of loose aggregates with parameters such as aggregate-size distribution, density, and dry stability simulated for the aggregates. After precipitation, the soil may evolve to a crusted surface with loose, erodible aggregates on the surface. The size distribution and total mass of these aggregates are simulated. Measurement techniques and field measurements for the latter have been reported (Potter, 1990; Zobeck, 1989).

Crust properties such as thickness and dry stability are also simulated. Strong crusts without loose material on top or an upwind abrader source are considered stable. Various processes, such as cultivation, may cause the soil surface to be composed of fractional areas of the two basic states. Modeling for WEPS of flat and standing cropland vegetation effects on wind erosion has also been reported (Hagen, 1996).

In WEPS, the temporal soil structural state is supplied to the erosion submodel by other submodels, while in most other models it is supplied by the user. However, the challenge is still to identify and quantify the total SSD. Loose suspension-size particles are one source of SSD. The smallest of these soil structural units, particles <0.01 mm in diameter, may comprise 2 to 3% of soil mass, but are typically <1% (Hagen et al., 1996) or may not be present as loose particles (Alfaro et al., 1997). These particles are characterized by interparticle cohesive forces that exceed the gravitational forces on the particle. Nevertheless, these cohesive forces are relatively weak and easily broken by saltation impacts to allow rapid entrainment into the air stream as demonstrated by wind tunnel experiments on clay particles (Shao and Raupach, 1993; Alfaro et al., 1997). Aggregates 0.01 to 0.10 mm in diameter comprise the bulk of the loose suspension-size soil available for the direct emission caused by saltation impacts, aided by aerodynamic forces. While the upper size limit on the total suspension component depends strictly on friction velocity and particle terminal velocity, we selected 0.10 mm for nominal use because in typical events these are only slightly effective

as surface abraders and only a minor portion are trapped in drifts at field boundaries (Chepil, 1957).

Potential additional sources of SSD include material from breakdown of saltating aggregates and material from abrasion of clods and crust. We made a distinction between these sources because saltation-size, water-stable aggregates have much higher dry stability than clods and crusts (Chepil, 1953). In addition, clods and crusts may be absent or covered with flat residues, while saltation-size particles are usually present during wind erosion. The total suspension component from wind erosion is modeled as the sum of the three sources: emission of loose SSD, breakage from saltating aggregates, and abrasion from clods and crust.

Suspension Flux from Emission of Loose Aggregates

In WEPS, the direct emission of SSD is calculated as a fraction of the net emission of total loose aggregates plus additional entrainment caused by mixing of the loose surface aggregates:

$$\mathrm{Gss}_{en} = \mathrm{SFss}_{en}\, C_{en}(q_{en} - q) + C_m q \qquad [2]$$

where Gss_{en} is the net vertical flux of suspension from emission of loose soil (kg m^{-2} s^{-1}), SFss_{en} is the soil fraction of suspension in emitted loose soil, C_{en} is the emission coefficient (m^{-1}), q_{en} is the transport capacity for saltation (kg m^{-1} s^{-1}) calculated using dynamic threshold friction velocity, q is the saltation discharge (kg m^{-1} s^{-1}), and C_m is a mixing entrainment coefficient (m^{-1}). A typical value of the emission coefficient for a bare, smooth, loose, and erodible soil is 0.06 m^{-1}, and values for other conditions have been reported (Hagen, 1995). The transport capacity for saltation can be expressed as (Greeley and Iversen, 1985)

$$q_{en} = C_s\, U_*^2\, (U_* - U_{*t}) \qquad [3]$$

where C_s is the saltation transport parameter (kg s^2 m^{-4}), with a typical value of about 0.3, which increases for surfaces armored with stones (Bagnold, 1943); U_* is the friction velocity (m s^{-1}); and U_{*t} is the dynamic threshold friction velocity (m s^{-1}), the threshold at which particle movement is sustained, described as (Bagnold, 1943)

$$U_{*t} = 0.8\, U_{*ts} \qquad [4]$$

where U_{*ts} is the static threshold friction velocity (m s^{-1}), the velocity at which numerous aggregates begin to move; for nonvegetated soil, it is a function of aerodynamic roughness and the soil areal fractions covered by both erodible soil and immobile fractions such as clods and crusts or rocks (Hagen, 1995; Marticorena et al., 1997). For a highly erodible surface, the threshold is $\approx$0.3 m s^{-1}.

An assumption inherent in the first term on the right-hand side of Eq. [2] is that the loose components of suspension and saltation- and creep-size aggregates occur as a uniform mixture in the field surface soil. As a consequence, we further assume that during simple net emission of these particles, the suspension fraction (SFss_{en}) remains the same as the suspension fraction in the soil. Hence, the suspension fraction of soil in the emitted loose soil can be estimated as (Hagen, 1995)

$$\mathrm{SFss}_{en} = \frac{\mathrm{SFss}}{\mathrm{SFer}} \qquad [5]$$

where SFss_{en} is the soil fraction of suspension in emitted loose soil, SFss is the suspension fraction of soil, and SFer is the erodible fraction of soil.

When saltation- and creep-size aggregates are ejected by saltation impacts at such low energy from the surface that they do not become part of the general saltation discharge, the term *reptation* has been applied to the movement of these aggregates (Anderson et al., 1991). However, when suspension-size particles are ejected at low energy by similar impacts, some of them probably move into suspension because transport capacity for this component is generally not limiting. The suspension rate of these aggregates is modeled in the second term on the right-hand side of Eq. [2]. The result of the latter process is to gradually deplete the loose suspension-size particles in the near-surface layer and leave coarser materials on the surface. Because the remaining small aggregates have relatively large surface area per unit mass, they tend to absorb most of the energy from saltation impacts. Thus, the process is rather self-limiting. Based on scaling considerations, an estimate for C_m is

$$C_m = 0.0001\ \mathrm{SFss}_{en} \qquad [6]$$

However, additional experimental research is needed to verify this estimate.

Generally, the soil fraction with aggregates <0.84 mm in diameter is considered the erodible fraction, and the fraction <0.10 mm is considered the suspension fraction. Hence, to estimate the erodible (SFer) and suspension (SFss) fractions of a selected soil for a range of conditions, the aggregate-size distribution of the soil should be determined. In this study, a modified four-parameter (Irani and Callis, 1963; Wagner and Ding, 1994) and a two-parameter (Hagen et al., 1987) lognormal distribution were compared for estimating the suspension fraction of soil samples. In a four-parameter, modified lognormal distribution, the percentage of mass greater than a specified diameter, d, is given by

$$P(\% \geq d) = 50 - 50\ \mathrm{erf}\left[\frac{\ln(d_x/d_g)}{\sqrt{2}\ \ln\sigma_g}\right] \qquad [7]$$

$$d_x = \frac{(d - d_o)\,(d_\infty - d_o)}{d_\infty - d} \qquad [8]$$

where d is the aggregate diameter (mm), d_g is the geometric mean diameter (mm), d_x is the modified aggregate size (mm), d_o is the minimum size of aggregates (mm), d_∞ is the maximum size of aggregates (mm), and σ_g is the geometric standard deviation. Replacing d_x with d in Eq. [7] results in the two-parameter lognormal distribution, which provides the percentage of mass greater than d (Hagen et al., 1987).

Suspension Flux from Abrasion of Clods and Crust

A second source of SSD is from abrasion of surface clods and crust by impacts of saltating aggregates that create and eject a range of aggregate sizes. Laboratory studies show that the total, vertical flux from abrasion of clods and crust can be described as (Hagen, 1991b)

$$G_{an} = \sum_{i=1}^{2} (F_{ani} C_{ani}) q \qquad [9]$$

where G_{an} is the vertical flux of aggregates abraded from clods and crust (kg m^{-2} s^{-1}), F_{ani} is the fraction of saltating aggregates impacting the ith target, C_{ani} is the abrasion coefficient of the ith target (clods or crust) (m^{-1}), and q is the saltation discharge (kg m^{-1} s^{-1}). The value of C_{ani} is independent of both the wind speed and magnitude of q (Hagen, 1991b). While the surface may be composed of additional impact targets, such as vegetation or rock, the C_{ani} for these is assumed negligible, so in most cases only the exposed clods and crusts need to be considered. A practical method to obtain C_{ani} from field soil samples was reported in an earlier study (Hagen et al., 1992), which

Table 1. Location, description, dispersed particle-size distribution, and organic matter content of 11 Kansas soils (Skidmore and Layton, 1992).

Location	Soil mapping unit	Taxonomic classification	Particle-size distribution			Organic matter
			Sand	Silt	Clay	
			g kg^{-1}			
Riley County (Manhattan)	Carr sandy loam	Coarse-loamy, mixed (calcareous), mesic Typic Udifluvent	588	355	55	11
Geary County (Topeka)	Eudora silt loam	Coarse-silty, mixed, smectitic Fluventic Hapludoll	291	545	164	15
Riley County (Manhattan)	Haynie silt loam	Coarse-silty, mixed (calcareous), mesic Mollic Udifluvent	337	584	87	19
Ellis County (Hays)	Harney silt loam	Fine, montmorillonitic, mesic Typic Argiustoll	98	611	293	14
Ellis County (Hays)	Inavale loamy sand	Sandy, mixed, mesic Typic Ustifluvent	815	126	59	8
Sherman County (Goodland)	Keith silt loam	Fine-silty, mixed, mesic Aridic Argiustoll	196	583	221	9
Geary County (Topeka)	Kimo silty clay loam	Clayey over loamy, smectitic mesic Fluvaquentic Hapludoll	200	440	360	22
Ellis County (Hays)	New Cambria silty clay loam	Fine, montmorillonitic, mesic Cumulic Haplustoll	143	466	391	26
Riley County (Manhattan)	Reading silt loam	Fine-silty, mixed, mesic Typic Argiudoll	64	701	236	23
Riley County (Manhattan)	Smolan silty clay loam	Fine, montmorillonitic, mesic Pachic Argiustoll	67	601	329	19
Riley County (Manhattan)	Wymore silty clay loam	Fine, montmorillonitic, mesic Aquic Argiudoll	78	638	284	24

demonstrated that abrasion coefficients could be predicted as a function of dry aggregate stability. Other work also showed that the mean and variance of the dry stability can be predicted from clay content (Skidmore and Layton, 1992). The value of F_{ani} is predicted using surface cover and roughness. The suspension flux from abrasion of clods and crust can be expressed as (Hagen, 1995)

$$\mathrm{Gss}_{an} = \mathrm{SFss}_{an} G_{an} \qquad [10]$$

where Gss_{an} is the suspension flux from abrasion of clods and crust (kg m^{-2} s^{-1}), and SFss_{an} is the soil fraction of material in suspension created during abrasion of clods and crust. In this study, the effect of soil textural properties on SFss_{an} of some Kansas soils was investigated.

Suspension Flux from Breakdown of Saltating Aggregates

A third source of suspension-size particles is from breakdown of saltating aggregates on impact at the soil surface or by collisions with each other during erosion events. The suspension flux from breakdown of saltating aggregates is simulated as (Hagen, 1995)

$$\mathrm{Gss}_{bk} = -C_{bk}\,(q - q_s) \qquad [11]$$

where Gss_{bk} is the suspension flux from breakdown of saltating aggregates (kg m^{-2} s^{-1}), C_{bk} is a breakage coefficient (m^{-1}), q is the saltation discharge (kg m^{-1} s^{-1}), and q_s is the saltation discharge in the form of primary sand particles. Solving Eq. [11] for q and C_{bk} gives

$$q = q_s + (q_o - q_s)\exp(-C_{bk}\,X) \qquad [12]$$

$$-C_{bk} = \frac{-1}{X \ln[(q - q_s)/(q_o - q_s)]} \qquad [13]$$

where q_o is the initial saltation discharge (kg m^{-1} s^{-1}) and X is the cumulative distance traveled by saltating aggregates. In this study, the effect of soil textural properties on C_{bk} was investigated. Finally, the total suspension flux is equal to the sum of the individual components:

$$\mathrm{Gss} = \mathrm{Gss}_{en} + \mathrm{Gss}_{an} + \mathrm{Gss}_{bk} \qquad [14]$$

MATERIALS AND METHODS

Suspension Fraction Available for Emission

Eleven Kansas soils with a wide textural range were sampled in the spring and fall of 1991 through 1994. The soil samples were taken from a surface layer of 0 to 20 and 20 to 200 mm. The samples were a 10-kg composite from five locations in each sample field. The descriptions and dispersed particle-size distribution of soil samples (Table 1) were adapted from Skidmore and Layton (1992). After air drying the soil samples, the fine fraction (<0.42 mm) was separated using 302-mm-diameter flat sieves. A sieve cover was used to ensure that fine particles did not escape into the air. A soil subsample of 2.0 g was then sieved using micromesh sieves (ATM Corporation, Sonic Sifter Division, Milwaukee, WI) to determine the fine end (<0.42 mm) of the aggregate-size distribution. The remainder of the soil samples were then sieved using a rotary sieve (Lyles et al., 1970) to determine the coarse end (>0.42 mm) of the aggregate-size distribution. The sieve cut fractions of both rotary and micromesh sieves were 0.010, 0.020, 0.030, 0.053, 0.075, 0.106, 0.150, 0.250, 0.420, 0.840, 2.0, 6.4, 19.0, 45.0, and 76.0 mm.

The sieving procedure was designed to overcome the weak interaggregate forces, but not the intraaggregate forces. In general, the large aggregates are the weakest and also subjected to the largest impact forces in the sieves. Hence, most breakage during the relatively short sieving times occurs in aggregates generally above the saltation size. While sieving is not perfect, it is a standard method used to successfully size aggregates down to ≈0.01 mm (Syvitski, 1991). For every soil sample, the four parameters, d_o, d, d_g, and σ_g were estimated by curve fitting Eq. [7] and [8] to the measured aggregate-size distribution. The four parameters then were used to predict the SFss (<0.10 mm) of soil samples. A two-parameter lognormal distribution was also used to predict SFss (<0.10 mm) of soil

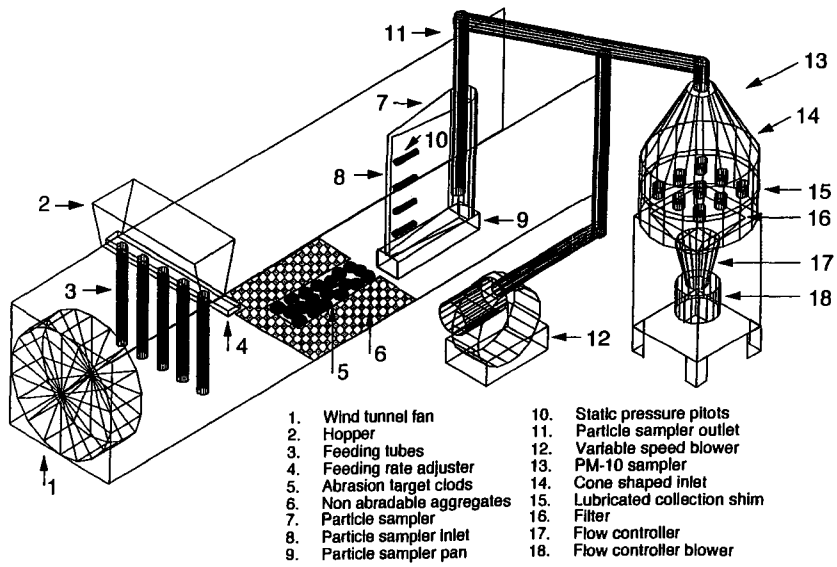

Fig. 3. Diagram of wind tunnel and sampling equipment used for clod abrasion tests.

samples. The soil fraction of suspension in emitted loose soil ($SFss_{en}$) was calculated by using the ratio of SFss to SFer. The relationship between dispersed particle-size distribution and loose suspension fraction of soil samples also was investigated.

Suspension Flux from Abrasion of Clods

This experiment was conducted using a nonrecirculating push-type wind tunnel equipped with particulate sampling equipment as denoted by item numbers and illustrated in Fig. 3. The wind tunnel was powered by a gasoline engine driving a constant-pitch fan (Fig. 3, no. 1). A short convergence section, screens, and a honeycomb after the fan were connected to a working section 12.2 m in length and 0.92 by 0.92 m in cross section.

Soil samples from the Ap horizon of Carr sandy loam, Haynie silt loam, Keith silt loam, and Wymore silty clay loam were collected from tilled fields in spring 1994. The descriptions of soil samples are given in Table 1. The soil samples were air dried, then their large aggregates (15–25 mm) were separated by rotary sieving (Lyles et al., 1970) and used as target aggregates. A 40 to 50% cover of soil aggregates (Fig. 3, no. 5) was placed on a 0.3 by 2.0 m wire mesh located 10.7 m downwind from the abrader inlets and in the front of the vertical particle sampler (Fig. 3, no. 7) in the wind tunnel. Nonabradable aggregates (lava rocks) were placed around the target aggregates (Fig. 3, no. 6).

Next, saltation-size sands, 0.29 to 0.42 mm in diameter, were washed, dried, and then placed in the hopper (Fig. 3, no. 2) located on top of the wind tunnel. After the fan in the wind tunnel was turned on, saltation-size sands were released down through the feeding tubes (Fig. 3, no. 3), which were extended from the hopper to 0.04 m above the tunnel floor. The feed rate of saltation-size sands was regulated by varying the size of adjustable openings (Fig. 3, no. 4) at the bottom of the hopper. Saltating sands were blown across the target aggregates at a free stream air velocity of 15 m s^{-1}.

A subsample of all soil moving down the tunnel was collected by a 3.8-mm-wide and 900-mm-tall vertical particle sampler (Fig. 3, no. 7) mounted at the tunnel outlet. Tests of the vertical particle sampler showed that the flow in the sampler was nearly isokinetic and the sampler was collecting suspended particles with >98% efficiency (Mirzamostafa, 1996). Where necessary, the data were corrected for sampler efficiency. A variable-speed blower (Fig. 3, no. 12) was adjusted to obtain isokinetic flow at the vertical particle sampler inlet (Fig. 3, no. 8) as indicated by four paired, interior and exterior, static pressure ports (Fig. 3, no. 10). Coarse particles were collected in the sampler pan (Fig. 3, no. 9), whereas fine particles moved upward through the sampler outlet (Fig. 3, no. 11). An isokinetic subsample ranging from 30 to 35% from outlet flow of the vertical particle sampler (Fig. 3, no. 11) was drawn into a high-volume PM_{10} sampler[1] (Fig. 3, no. 13; Andersen-Graseby Model 1200, Graseby Andersen, Atlanta, GA) fitted with a cone-shaped inlet (Fig. 3, no. 14). Particles larger than PM_{10} were collected on a lubricated collection shim (Fig. 3, no. 15), and PM_{10} particles were collected on a filter (Whatman quartz microfiber filter, Fig. 3, no. 16). Filters were dried and weighed before and after collection runs of 10 to 20 min. A flow controller (Fig. 3, no. 17) and an attached blower (Fig. 3, no. 18) ensured a constant flow to the sampler.

After each run, the target aggregates on the wire mesh were reweighed, and the abraded loss per unit of tunnel floor area was calculated. There were two replications for every soil sample. The results were used to investigate the effect of soil textural properties on the abrasion coefficient (C_{an}) and soil fraction of suspension created during abrasion of clods ($SFss_{an}$), which were calculated as follows

$$C_{an} = \frac{M_{an}/L_{an}}{M_{st}} \quad [15]$$

$$M_{an} = M_{agi} - M_{agf} \quad [16]$$

$$SFss_{an} = \frac{M_{sus}(W_{target}/W_{sampler})}{M_{an}} \quad [17]$$

where L_{an} is the length along the wind direction of the target area with 40 to 50% aggregate cover (m), M_{agf} is the final mass of target aggregates (g), M_{agi} is the initial mass of target aggregates (g), M_{an} is the abrasion mass from target aggregates (g), M_{sf} is the mass of saltating sands fed into the wind tunnel (g), M_{st} is the mass of saltating sands passing the target aggregates (g), M_{sus} is the mass of SSD abraded from target and caught by the vertical particle sampler, $W_{sampler}$ is the width of

[1] Mention of product names is for information purposes and does not imply endorsement by the authors.

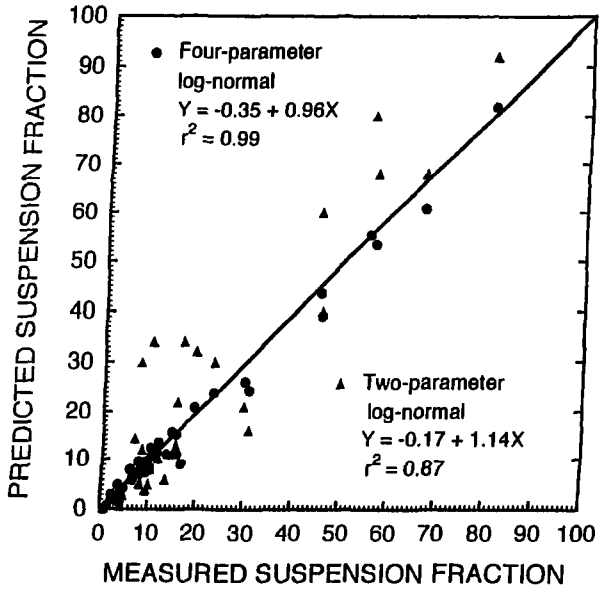

Fig. 4. A comparison of measured and predicted suspension fractions (<0.106 mm) in 11 Kansas soils using four-parameter and two-parameter lognormal distributions.

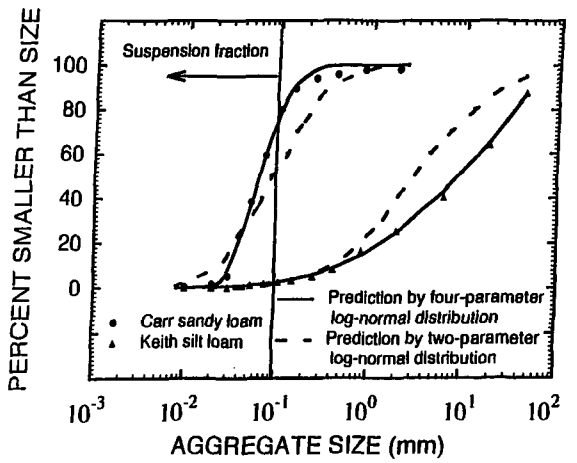

Fig. 5. Measured and predicted aggregate-size distributions of Carr sandy loam and Keith silt loam using two-parameter and four-parameter lognormal distributions.

the vertical particle sampler (3.8 mm), and W_{target} is the width of the target aggregates (300 mm).

Suspension Flux from Breakdown of Saltating Aggregates

In this experiment, four soil samples from the Ap horizon of Carr sandy loam, Haynie silt loam, Keith silt loam, and Wymore silty clay loam were collected from the surface of tilled fields in spring 1994. The soil samples were air dried and rotary sieved to prepare saltation-size aggregates with sizes of 0.15 to 0.42 and 0.42 to 0.84 mm.

The wind tunnel setup (Fig. 3) in this experiment was similar to that described above, except no target clods were used. Each type of saltating aggregate was fed into the upwind hopper tubes and exited near the bare plywood floor of the wind tunnel. The saltating aggregates then moved along the bare plywood floor and were collected on a tarp in the outlet bin, weighed, and again recycled down the tunnel at a free stream air velocity of 13 m s^{-1}. This process was repeated until the saltating aggregates had traveled about 300 m down the tunnel. Fine particles created during breakdown of saltating aggregates in the wind tunnel were collected by the vertical and PM_{10} sampler located at the end of the tunnel. Regression on Eq. [12] was used to calculate the coefficient of breakage (C_{bk}) of saltating aggregates in the wind tunnel. The effect of soil textural properties on C_{bk} also was investigated.

RESULTS AND DISCUSSION

Suspension Fraction Available for Direct Emission

The measured suspension fraction obtained by sieving vs. the suspension fractions estimated by both lognormal distributions are plotted in Fig. 4. The hypotheses that the intercept equals zero for both regression equations were not rejected at $P < 0.05$. The hypothesis that slope equals one for the regression equation of four-parameter lognormal distribution was not rejected at $P < 0.05$. However, the hypothesis that slope equals one for the regression equation of two-parameter lognormal distribution was rejected at $P < 0.05$. Additionally, the r^2 for the suspension fraction estimated by a modified, four-parameter lognormal distribution (0.99) was higher than the r^2 for the two-parameter lognormal distribution (0.87). Thus, the loose suspension fraction of a soil can be estimated more accurately from the modified, four-parameter lognormal distribution. This result occurs because soils with a significant sand content tend to deviate from a true lognormal distribution, as illustrated by data from the Carr and Keith soils in Fig. 5. Hence, when evaluating soils to determine the available, loose suspension component and other components, it is important to sieve the entire size range and then select a distribution capable of describing the size range when reporting the data.

These results also agree with the earlier conclusion by Wagner and Ding (1994) that aggregate-size distribution of a soil can be simulated by a modified, four-parameter lognormal distribution. However, their finding was based on evaluation of only one soil (Reading silt loam).

The use of an aggregate-size distribution is necessary to model a variable suspension fraction as a function of wind friction velocity. To implement this procedure, however, additional research is needed to accurately simulate the four parameters of the distributions based on intrinsic soil properties, soil management, and weather.

A less stringent approach is to select a single size cut for the available suspension component and then develop predictions for it. The mean suspension fractions (<0.1 mm) of 11 Kansas soils ranged from 0.05 (Kimo silty clay loam) to 0.64 (Carr sandy loam) in the 0- to 20-mm layer, and from 0.03 (Kimo silty clay loam) to 0.51 (Carr sandy loam) in the 20- to 200-mm layer. The mean suspension fractions in the 0- to 20-mm layer was significantly higher than the mean suspension fraction in the 20- to 200-mm layer at $P < 0.05$. The mean suspension fraction of soil samples was observed to be directly proportional to the ratio of (silt + sand [0.05–0.1 mm])/clay, with $r^2 = 0.87$ for 0 to 20 mm and $r^2 = 0.84$

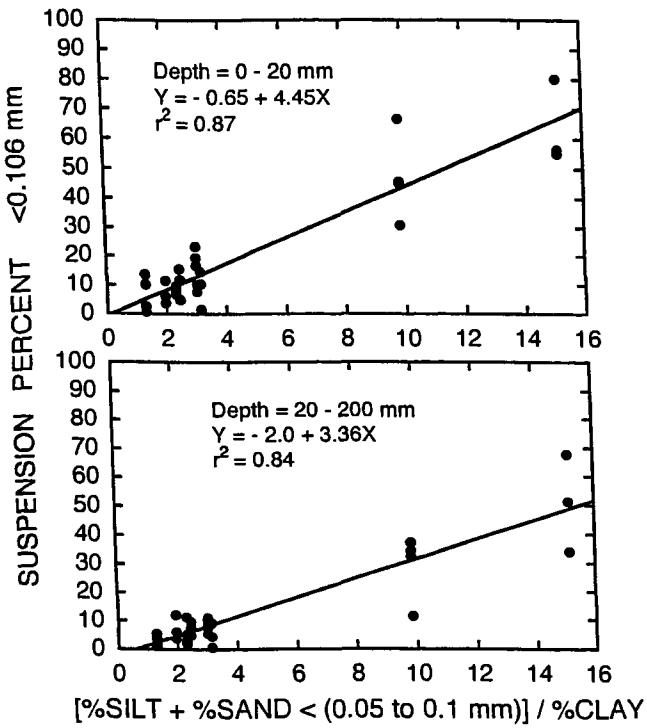

Fig. 6. Relationship between suspension (<0.106 mm) and ratio of (silt + sand <0.10 mm)/clay in 11 Kansas soils.

for the 20- to 200-mm soil layer at $P < 0.05$ (Fig. 6). This result suggests that the dispersed particle-size distribution can be used to estimate a single-valued, loose, suspension fraction of a soil.

However, the linear prediction equations in Fig. 6 represent only part of the range of soils and do not account for deviations from the mean caused by freeze–thaw and other effects. Thus, the predictions illustrated in Fig. 6 should not be extrapolated beyond the range of the data. Many additional soils are currently being tested to extend the data range, which will probably result in a nonlinear function. In WEPS, intrinsic soil properties are used to establish a predicted mean and variance of the dependent temporal soil variable for each soil layer; then simulated management and weathering processes are used to drive the dependent variable within the predicted range.

The mean suspension fractions in the loose erodible

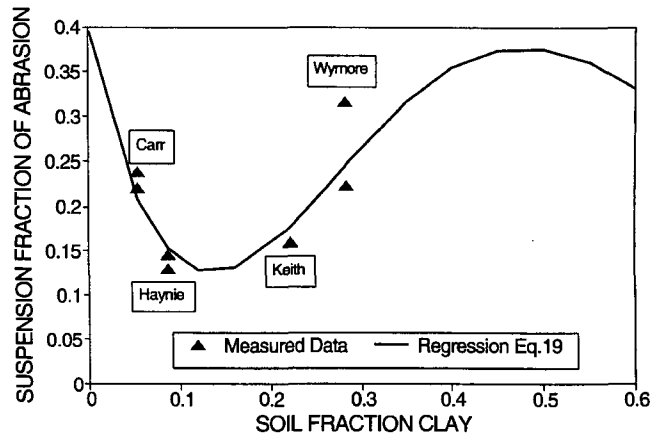

Fig. 7. Fraction of suspension-size aggregates created during clod abrasion of four Kansas soils.

fractions ($SFss_{en}$) of four Kansas soils ranged from 0.19 (Keith silt loam) to 0.69 (Carr sandy loam) (Table 2). The $SFss_{en}$ represents nearly the minimum ratio of suspension discharge to downwind saltation discharge because other processes also contribute to the suspension component.

Suspension Flux from Abrasion of Clods

The abrasion coefficients (C_{an}) for four Kansas soils are shown in Table 2. The abrasion coefficients ranged from 0.1064 m^{-1} (Carr sandy loam) to 0.0018 m^{-1} (Wymore silty clay loam). The abrasion coefficients of Carr and Haynie soils exceeded those of Keith and Wymore soils by 13 to 59 times.

The mean soil fractions of suspension created during abrasion of clods ($SFss_{an}$) for four Kansas soils are also shown in Table 2. The range of the mean $SFss_{an}$ was from 0.14 (Haynie silt loam) to 0.27 (Wymore silty clay loam). Analysis of variance showed a statistically significant difference ($P < 0.001$) in the mean values among the soils. The data on the suspension fraction from clod abrasion (Fig. 7) suggest that, as clay content increases (Carr to Haynie), the suspension fraction of abrasion decreases. However, with a further increase of clay content (Haynie to Wymore), the suspension fraction of abrasion increases.

The range of C_{an} measured on the four tested soils

Table 2. Measured values of emission, abrasion, and breakage coefficients† for four Kansas soils.

Soil mapping unit	Emission			Abrasion		Breakage	
	SFer‡	SFss	$SFss_{en}$	C_{an}	$SFss_{an}$	C_{bk1}	C_{bk2}
				m^{-1}		m^{-1}	
Carr sandy loam	0.92 (0.06)†	0.64 (0.14)	0.69 (0.12)	0.1064 (0.0237)	0.23 (0.01)	0.0139	–§
Haynie silt loam	0.72 (0.12)	0.47 (0.15)	0.66 (0.09)	0.0508 (0.0029)	0.14 (0.01)	0.0091	0.0088
Keith silt loam	0.45 (0.41)	0.09 (0.09)	0.19 (0.03)	0.0038 (0.0001)	0.16 (0.00)	0.0029	0.0013
Wymore silty clay loam	0.44 (0.19)	0.11 (0.05)	0.24 (0.03)	0.0018 (0.0002)	0.27 (0.07)	0.0027	0.0014

† SFer, erodible fraction (<0.84 mm); SFss, suspension fraction (<0.10 mm); $SFss_{en}$, suspension fraction in the loose erodible fraction; C_{an}, abrasion coefficient; $SFss_{an}$, suspension fraction created by clod abrasion; C_{bk1}, brakage coefficient for aggregate size of 0.15 to 0.42 mm; C_{bk2}, breakage coefficient for aggregate size of 0.42 to 0.84 mm.
‡ Means with standard deviation in parentheses.
§ Data are not available.

was wide and covered the range typically observed in soils (Hagen et al., 1992). In contrast, the measured suspension fractions of abraded soil fell within a relatively narrow range, but varied nonlinearly with clay content. A regression equation with reasonable behavior across a wider range, but fitted to these limited data ($r^2 = 0.69$), is

$$SFss_{an} = 0.40 - 4.825SF_{cla} + 27.185SF_{cla}^2 - 53.695SF_{cla}^3 + 42.209SF_{cla}^4 - 10.70SF_{cla}^5 \quad [18]$$

where SF_{cla} is soil fraction clay.

One possible explanation of the result may be that coarse-textured soils such as Carr sandy loam, which contain a large fraction of fine sands (47%), have the most unstable aggregates, which are most susceptible to abrasion. Thus, during abrasion of these soil aggregates, a significant fraction of abraded materials would be in the form of suspension-size fine sand particles. As the soil texture becomes finer, like Haynie silt loam, the aggregates become more stable. Thus, during abrasion of these soil aggregates, the abraded material would be in larger fragments, so the suspension fraction of abrasion ($SFss_{an}$) will be smaller than that of the Carr sandy loam soil. However, with a further increase in clay content (Wymore silty clay loam), the total abrasion from aggregates decreases, but the abraded material tends to be in smaller fragments, thus producing an increase in the fractions of SSD.

Suspension Flux from Breakdown of Saltating Aggregates

The breakdown of saltating aggregates during wind erosion is a complex process. However, prior laboratory chamber studies on effects of impacts on saltation-size aggregates demonstrated that they break down and yield significant amounts of SSD (Hagen and Lyles, 1985; Singh et al., 1994). Another variable in the field is that the saltation impact sites may range from other loose aggregates to desert pavement. To assess the importance of the impact surface, preliminary breakdown tests were conducted using rocks, straw, and plywood as impact surfaces. The results showed no differences in breakage among these surfaces at $P < 0.05$ (Mirzamostafa, 1996). In the case where loose aggregate is the impact surface, the WEPS model (Hagen, 1995) assumes that the SSD from breakage of both impacting and surface aggregates equals the breakage from impacts of saltating aggregates on solid surfaces. However, this assumption may require additional validation.

A further complication occurs because wind tunnel tracer tests over loose surfaces demonstrate that saltating aggregates frequently are replaced by new saltating aggregates from the soil surface (Willetts and Rice, 1985). Hence, saltating aggregates moving at any point in a field probably have traveled various distances and been subjected to a different number of impacts. Although travel distance of saltating aggregates was controlled in the present wind tunnel experiments, to cope with the general field case of unknown travel distances, a constant breakage coefficient for each soil was postulated above (Eq. [11]). Fortunately, the measured data supported this assumption.

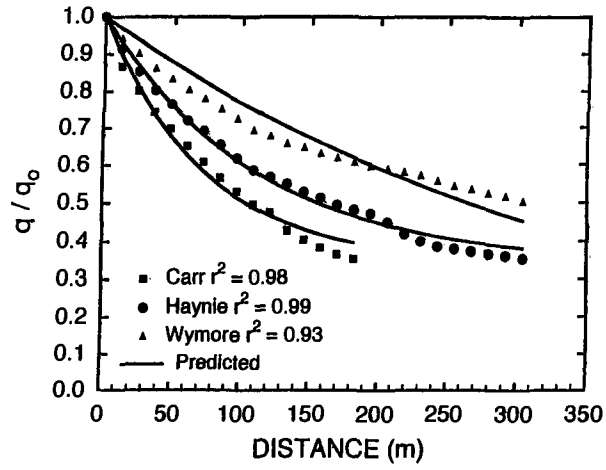

Fig. 8. Predicted and observed saltating aggregate discharge (0.15–0.42-mm diameter) vs. distance for Carr sandy loam, Haynie silt loam, and Wymore silty clay loam.

A series of constant breakage coefficients (Eq. [11]) provided good fits to the measured breakage data, with $r^2 > 0.93$ for all the tested soils (Fig. 8). The range of breakage coefficients of saltating aggregates with sizes of 0.15 to 0.42 mm was from 0.0139 m^{-1} (Carr sandy loam) to 0.0027 m^{-1} (Wymore silty clay loam). The breakage coefficients of Carr and Haynie soils (0.15–0.42 mm) exceeded those of Keith and Wymore soils by three to five times (Table 2). The range of breakage coefficient of saltating aggregates with sizes of 0.42 to 0.84 mm was from 0.0088 (Carr sandy loam) to 0.0013 m^{-1} (Keith silt loam). The breakage coefficient of Carr (0.42 to 0.84 mm) exceeded those of Keith and Wymore soils by six times (Table 2).

We observed that the breakage coefficient of saltating aggregates is inversely proportional to clay fraction, with $r^2 = 0.961$ (Fig. 9), and directly proportional to the abrasion coefficient, with $r^2 = 0.989$ at $P < 0.05$ (Fig. 10). The results show that abrasion coefficients are about nine times higher than breakage coefficients for the tested soils.

The dispersed particle-size distribution of saltating aggregates was determined using the pipette method (Gee and Bauder, 1986) before and after saltation in

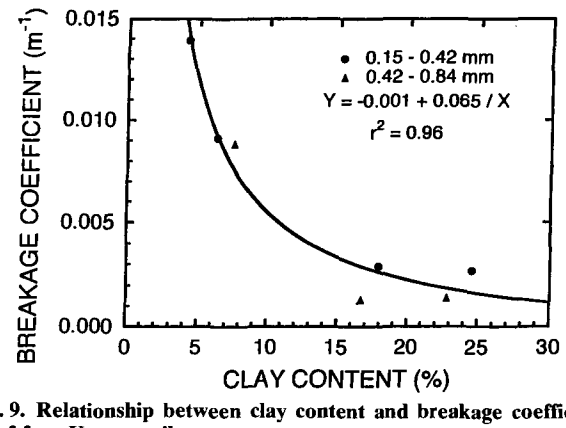

Fig. 9. Relationship between clay content and breakage coefficient of four Kansas soils.

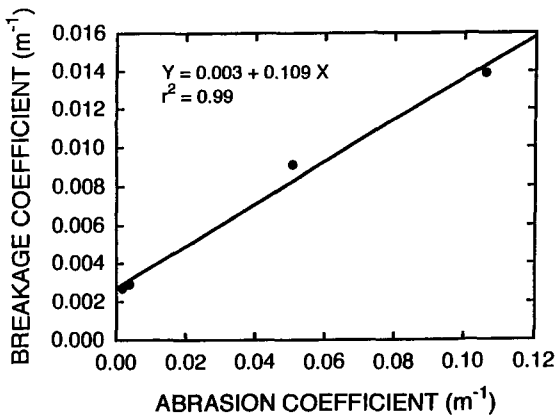

Fig. 10. Relationship between breakage coefficient and abrasion coefficient of four Kansas soils.

the wind tunnel (Table 3). The results showed that Carr and Haynie soils, which had the highest breakage coefficients, had 175 and 269 g kg^{-1} reductions in the silt fraction and 194 and 301 g kg^{-1} increases in the sand fraction, respectively. However, the change in texture of finer textured soils, such as Keith and Wymore, was not as great as the change in coarser textured soils, such as the Carr and Haynie soils. The preferential breakdown of silt particles from soil aggregates during erosion also was observed by Lyles and Tatarko (1986).

In this study, a nominal diameter of 0.10 mm was selected as the boundary between saltation and SSD aggregates. However, we would reiterate that the boundary diameter between transport modes is a function of friction velocity. Hence, the ratio of suspension flux to saltation discharge may also vary with friction velocity. The SSD model presented here could be easily extended to accommodate this change to improve model accuracy. However, to make the improved accuracy a reality, we must first improve our ability to predict and measure the short-term aggregate-size distributions both at the surface and above it during dust storms for a wide range of soils.

Overall, the suspension component of wind erosion is particularly important on large, uniform fields. On these fields the saltation discharge often approaches transport capacity and then does not increase downwind over much of the field. However, the transport capacity for the suspension component is much larger than that for saltation and is generally not exceeded. Hence over the entire field, breakage of saltating aggregates and, if they are present, abrasion from clods and crust contribute to the suspension component. These processes cause the suspension component to continually increase downwind. Measurements of the vertical suspension profiles in dust storms (Chepil and Woodruff, 1957) confirms that the suspension component of discharge often exceeds the saltation discharge. Relatively large source areas, such as Owen's (dry) Lake, California, generate large suspension components. Based on vertical flux measurements at Owen's Lake, one may conclude that, at the downwind boundary, discharge of even the finest component of suspension, the PM_{10}, readily exceeds the saltation and creep discharge (Gillette et al., 1998).

CONCLUSIONS

Three major sources of the suspension component of wind erosion were identified: emission of loose suspension-size aggregates, abrasion from clods and crust, and breakage of saltating aggregates. Based on conservation of mass and other physical principles, model equations were presented that can be used to account for the SSD from each of these individual sources. There are potential advantages in simulating SSD from individual sources as opposed to treating the soil as a lumped source. These include the ability to develop physically based equations to update soil surface conditions in response to erosion, distinguish differences in SSD generation as soil structure or cover of flat residues change, and better understand the relationships among the physical processes. One example illustrates the latter point. Breakage and subsequent suspension of the saltation and creep aggregates forces a continual need to emit additional saltation-size aggregates from the surface to satisfy equilibrium conditions. There are then two consequences usually not considered: saltation discharge must remain below transport capacity in order to drive the emission, and net emission of saltation-size aggregates occurs over the entire field.

In portions of a typical eroding field where saltation transport capacity far exceeds local saltation discharge, direct emission of loose aggregates is the dominant suspension source. In 11 Kansas soils tested, the suspension fraction (<0.10 mm), of the loose erodible fraction (<0.84 mm) ranged from 0.19 (Keith silt loam) to 0.69 (Carr sandy loam). These values probably represent the minimum values of downwind suspension discharge relative to saltation discharge for these soils because

Table 3. Effect of saltation on dispersed primary particle-size distribution of soil abraders.

Soil series	Abrader size	Before saltation			After saltation			Fraction changed		
		Sand >0.05 mm	Silt 0.002–0.05 mm	Clay <0.002 mm	Sand >0.05 mm	Silt 0.002–0.05 mm	Clay <0.002 mm	Sand >0.05 mm	Silt 0.002–0.05 mm	Clay <0.002 mm
	mm	g kg^{-1}								
Carr	0.15–0.42	778	179	43	973	4	24	194	−175	−19
Haynie	0.15–0.42	639	298	63	940	29	31	301	−269	−32
Keith	0.15–0.42	189	631	179	157	653	191	−33	21	12
Wymore	0.15–0.42	110	644	246	104	658	238	−6	14	−8
Haynie	0.42–0.84	550	375	76	780	162	58	231	−213	−18
Keith	0.42–0.84	160	673	167	156	644	200	−4	−29	33
Wymore	0.42–0.84	85	687	228	83	676	241	−2	−11	13

additional suspension components are generated by other sources.

The mean fraction of loose, suspension-size soil can be predicted ($r^2 = 0.87$) from the dispersed particle-size distribution of Kansas field soils. However, additional data on other soils are needed to expand the range. Ultimately, in order to model a variable suspension fraction as a function of wind friction velocity or degradation of aggregates by abrasion, simulation of the complete aggregate-size distribution is needed. For this purpose, the results demonstrated that a two-parameter lognormal distribution was not adequate, and that a four-parameter, modified lognormal distribution was needed to accurately represent the loose suspension component in Kansas soils.

In wind tunnel tests, the surface clods from four Kansas soils were much weaker than the saltation-size aggregates of the same soils. Tests showed that the clod abrasion coefficients were about nine times higher than the breakage coefficients of saltating aggregates, but directly proportional to them. Although the clod abrasion coefficients covered a wide range, the suspension fraction of the soil abraded from clods remained in a surprisingly narrow range of 0.14 to 0.27. Hence, for a surface covered with at least 30 to 40% immobile clods, the suspension flux from clod abrasion will exceed the suspension flux from breakage of saltating aggregates.

The results also demonstrated that constant breakage coefficients could be used to represent breakage of saltating aggregates, at least for downwind travel distances of 300 m. On portions of an eroding field armored with rock or covered with loose saltating aggregates, this source can become dominant. During breakage, depletion of the silt fraction from the saltating aggregates was significantly higher in the sandy soils than in the finer textured soils. The latter result suggests that wind erosion will deplete the productivity of sandy soils faster than it will deplete the productivity of fine-textured soils.

The suspension flux from each of the three sources will vary, depending on the particular field. However, the transport capacity for suspension discharge is generally not exceeded on cropland fields. Hence, on a uniform field the suspension component of discharge should continually increase downwind because breakage of saltating aggregates, emission, and, if they are present, abrasion from clods and crust contribute to the suspension component over the entire field.

ACKNOWLEDGMENTS

We thank Mr. Wayne Carstenson and Mr. Andrew Hawkins for technical assistance in construction of sampling instruments and conducting wind tunnel experiments.

REFERENCES

Alfaro, S.C., A. Gaudichet, L. Gomes, and M. Maille. 1997. Modeling the size distribution of a soil aerosol produced by sandblasting. J. Geophys. Res. 102(D10):11239–11249.

Anderson, R.S., M. Sorenson, and B.B. Willetts. 1991. A review of recent progress in our understanding of aeolian sediment transport. Acta Mech. (Suppl.) 1:1–19.

Bagnold, R.A. 1943. The physics of blown sand and desert dunes. Chapman & Hall, London.

Cahill, T.A., T.E. Gill, J.S. Reid, E.A. Gearhart, and D.A. Gillette. 1996. Saltating particles, playa crusts, and dust aerosols at Owens (dry) Lake, California. Earth Surf. Processes Landforms 21: 621–639.

California Air Resources Board. 1991. Methods for assessing area source emissions in California. Calif. Environ. Protection Agency Emissions Inventory Branch Tech. Support Div., Sacramento.

Chepil, W.S. 1953. Field structure of cultivated soils with special reference to erodibility by wind. Soil Sci. Soc. Am. Proc. 17:185–190.

Chepil, W.S. 1957. Sedimentary characteristics of dust storms: I. Sorting of wind-eroded soil material. Am. J. Sci. 255:12–22.

Chepil, W.S., and N.P. Woodruff. 1957. Sedimentary characteristics of dust storms: II. Visibility and dust concentration. Am. J. Sci. 225:104–114.

Clark, E.H., J.A. Haverkamp, and W. Chapman. 1985. Eroding soils: The off-farm impacts. Conserv. Foundation, Washington, DC

Dregne, H.E. 1976. Soils of the arid regions. Elsevier, New York.

Gee, G.W., and J.W. Bauder. 1986. Particle-size analysis. p. 383–411. *In* A. Klute (ed.) Methods of soil analysis. Part 1. 2nd ed. Agron. Monogr. 9. ASA and SSSA, Madison, WI.

Gillette, D.A. 1977. Fine particulate emissions due to wind erosion. Trans. ASAE 20:890–897.

Gillette, D.A., D.W. Fryrear, T.E. Gill, T. Ley, T.A. Cahill, and E.A. Gearhart. 1998. Relation of vertical flux of particles smaller than 10 μm to total aeolian horizontal mass flux at Owens Lake. J. Geophys. Res. 102(D22):26009–26015.

Gillette, D.A., and R. Passi. 1988. Modeling dust emission caused by wind erosion. J. Geophys. Res. 93:14233–14242.

Gore, R. 1979. The desert: An age old challenge grows. Natl. Geogr. 156:594–639.

Greeley, R., and J.D. Iversen. 1985. Wind as a geological process. Cambridge Univ. Press, New York.

Hagen, L.J. 1991a. A wind erosion prediction system to meet user needs. J. Soil Water Conserv. 46:106–111.

Hagen, L.J. 1991b. Wind erosion mechanics: Abrasion of aggregated soil. Trans. ASAE 34:831–837.

Hagen, L.J. 1995. Erosion submodel technical description. p. E1–E49. *In* Proc. WEPP/WEPS Symp., Des Moines, IA. 10–11 Aug. 1995. Soil Water Conserv. Soc., Ankeny, IA.

Hagen, L.J. 1996. Crop residue effects on aerodynamic processes and wind erosion. Theor. Appl. Climatol. 54:39–46.

Hagen, L.J., and L. Lyles. 1985. Amount and nutrient content of particles produced by soil aggregate abrasion. p. 117–129. *In* Erosion and soil productivity. ASAE Publ. 8-85. Am. Soc. Agric. Eng., St. Joseph, MI.

Hagen, L.J., N. Mirzamostafa, and A. Hawkins. 1996. PM_{10} generation by wind erosion. p. 79–86. *In* Int. Conf. Air Pollut. Agric. Operations, Kansas City, MO. 7–9 Feb. 1996. Midwest Plan Serv., Ames, IA.

Hagen, L.J., E.L. Skidmore, and D.W. Fryrear. 1987. Using two sieves to characterize dry soil aggregate size distribution. Trans. ASAE 30:162–165.

Hagen, L.J., E.L. Skidmore, and A. Saleh. 1992. Wind erosion: Prediction of aggregate abrasion coefficients. Trans. ASAE 35:1847–1850.

Irani, R.R., and C.F. Callis. 1963. Particle size: Measurement, interpretation, and application. John Wiley & Sons, New York.

Lyles, L., J.D. Dickerson, and L.A. Disrud. 1970. Modified rotary sieve for improved accuracy. Soil Sci. 109:207–210.

Lyles, L., and J. Tatarko. 1986. Wind erosion effects on soil texture and organic matter. J. Soil Water Conserv. 41:191–193.

Marticorena, B., and G. Bergametti. 1995. Modeling the atmospheric dust cycle: 1. Design of a soil-derived dust emission scheme. J. Geophys. Res. 100(D8):16415–16430.

Marticorena, B., G. Bergametti, and B. Aumont. 1997. Modeling the atmospheric dust cycle 2. Simulation of Saharan dust sources. J. Geophys. Res. 102(D4):4387–4404.

Marticorena, B., G. Bergametti, D. Gillette, and J. Belnap. 1997. Factors controlling threshold friction velocity in semiarid and arid areas of the United States. J. Geophys. Res. 102(D19):23277–23287.

Mirzamostafa, N. 1996. Suspension component of wind erosion. Ph.D. diss. Kansas State Univ., Manhattan (Diss. Abstr. 9714341).

Oldeman, L.R. 1991. Global extent of soil degradation. p. 19–36. *In* Bi-annual report. Int. Soil Reference and Information Center, Wageningen, the Netherlands.

Piper, S.L. 1989. Measuring the particulate pollution damages from wind erosion in the western United States. J. Soil Water Conserv. 44:70–74.

Potter, K.N. 1990. Estimating wind-erodible materials on newly crusted soils. Soil Sci. 150:771–776.

Pye, K. 1987. Aeolian dust and dust deposition. Academic Press, London.

Shao, Y., and M.R. Raupach. 1993. Effect of saltation bombardment on the entrainment of dust by wind. J. Geophys. Res. 98(D7):12719–12726.

Shao, Y., M.R. Raupach, and J.F. Leys. 1996. A model for predicting aeolian sand drift and dust entrainment on scales from paddock to region. Aust. J. Soil Res. 34:309–342.

Singh, U.B., J.M. Gregory, G.R. Wilson, and T.M. Zobeck. 1994. Dust emission from a controlled energy environment. ASAE Pap. 944041. Am. Soc. Agric. Eng., St. Joseph, MI.

Skidmore, E.L., and J.B. Layton. 1992. Dry-soil aggregate stability as influenced by selected soil properties. Soil Sci. Soc. Am. J. 56: 557–561.

Syvitski, J.P. 1991. Principles, methods, and application of particle size analysis. Cambridge Univ. Press, New York.

U.S. Department of Agriculture. 1989. The second RCA appraisal: Soil, water, and related resources on nonfederal land in the United States. U.S. Gov. Print. Office, Washington, DC.

Wagner, L.E., and D. Ding. 1994. Representing aggregate size distributions as modified lognormal distribution. Trans. ASAE 37:815–821.

Willetts, B.B., and M.A. Rice. 1985. Inter-saltation collisions. p. 83–101. *In* O.E. Barndorff-Nielsen et al. (ed.) Proc. Int. Worksh. on the physics of blown sand, Aarhus, Denmark. 28–31 May 1985. Univ. of Aarhus, Aarhus, Denmark.

Woodruff, N.P., and F.H. Siddoway. 1965. A wind erosion equation. Soil Sci. Soc. Am. Proc. 29:602–608.

Zobeck, T.M. 1989. Fast-Vac — A vacuum system to rapidly sample loose granular material. Trans. ASAE 32:1316–1318.

Zobeck, T.M., and D.W. Fryrear. 1986. Chemical and physical characteristics of windblown sediment. II. Chemical characteristics and total soil and nutrient discharge. Trans. ASAE 29:1037–1041.